Orientation of β-Barrel Proteins OmpA and FhuA in Lipid Membranes. Chain Length Dependence from Infrared Dichroism†

Muthu Ramakrishnan,‡ Jian Qu,§ Cosmin L. Pocanschi,§ Jörg H. Kleinschmidt,*,§ and Derek Marsh*,‡

Max-Planck-Institut für biophysikalische Chemie, Abt. Spektroskopie, 37070 Göttingen, Germany, and Universität Konstanz, Fachbereich Biologie, 78547 Konstanz, Germany

ABSTRACT: The outer-membrane proteins OmpA and FhuA of *Escherichia coli* are monomeric β-barrels of widely differing size. Polarized attenuated total reflection infrared spectroscopy has been used to determine the orientation of the β-barrels in phosphatidylcholine host matrices of different lipid chain lengths. The linear dichroism of the amide I band from OmpA and FhuA in hydrated membranes generally increases with increasing chain length from diC(12:0) to diC(17:0) phosphatidylcholine, in both the fluid and gel phases. Measurements of the amide I and amide II dichroism from dry samples are used to deduce the strand tilt ($\beta = 46°$ for OmpA and $\beta = 44.5°$ for FhuA). These values are then used to deduce the order parameters, $\langle P_2(\cos \alpha) \rangle$, of the β-barrels from the amide I dichroic ratios of the hydrated membranes. The orientational ordering of the β-barrels and their assembly in the membrane are discussed in terms of hydrophobic matching with the lipid chains.

The integral proteins of the outer membrane of Gram-negative bacteria perform a variety of functions, including those of receptors, lipases, passive diffusion pores, sugar transport pores, and ligand-gated transport systems. Despite the diversity in function, the outer-membrane proteins are mainly, if not exclusively, of the β-barrel type: the second structural paradigm, in addition to the α-helix, for trans-membrane proteins. The size of the β-barrel ranges from 8 to 22 strands, the shear number of the barrel ranges from 8 to 24, and the degree of oligomerization varies from monomer to trimer (for a review, see ref *1*). The β-strands are tilted relative to the barrel axis by 36−42° (*2*). This structural information is obtained mostly from X-ray diffraction of crystals produced from purified proteins in detergent (*3−14*), and to a much lesser extent from solution-state NMR of proteins in detergent micelles (*15−18*). These environments approximate those of the lipid bilayer in biological membranes but do not provide information on the orientation of the β-barrel proteins in the membrane. The latter feature not only determines the way in which the protein is integrated into the membrane but also might be responsible, at least partly, for the functional differentiation between the various β-barrel proteins.

In principle, the dichroism of the amide bands in the infrared spectra from aligned membranes can be used to determine both the β-strand tilt and the orientation of the β-sheet plane or β-barrel axis (*19*, *20*). Combination of the dichroism from amide I and amide II bands allows deter-mination of both orientational parameters. If the strand tilt is known from X-ray diffraction, only one dichroic ratio is required to determine the orientation of the β-sheet or β-barrel. Several previous analyses of infrared dichroism from β-barrel membrane proteins have not exploited this possibility (*21−23*). Recently, this method of analysis has been applied successfully to ATR-FTIR studies on two isoforms of the voltage-dependent anion-selective channel (VDAC) from the outer membrane of mitochondria (*24*).

In the present work, we investigate the dependence on lipid chain length of the orientational tilt of two β-barrel trans-membrane proteins with very different sizes. One of these outer-membrane proteins from *Escherichia coli* is OmpA,[1] which has 8 β-strands; the other is the β-barrel domain of the ferrichrome−iron receptor FhuA mutant without the cork domain, which has 22 β-strands. Both proteins are monomers and, therefore, are those most likely to respond to the lipid environment. The β-barrel orientation displays a character-istic dependence on the lipid chain length that is determined by the hydrophobic span of the outer-membrane proteins and correlates well with the lipid requirement for spontaneous membrane insertion of OmpA (*25*).

THEORETICAL BACKGROUND

The order parameter, $\langle P_2(\cos \alpha) \rangle$, for the axis of a β-barrel protein with a circular cross section is related to the amide

---

* To whom correspondence should be addressed. Telephone: +49-551-201 1285. Fax: +49-551-201 1501. E-mail: dmarsh@gwdg.de (D.M.). Telephone: +49-7531 88 3360. Fax: +49-7531 88 3183. E-mail: joerg.helmut.kleinschmidt@uni-konstanz.de (J.H.K.).
‡ Max-Planck-Institut für biophysikalische Chemie.
§ Universität Konstanz.
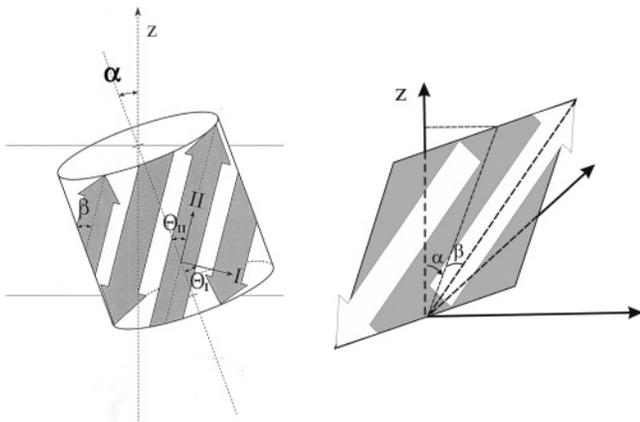
FIGURE 1: Orientation of transition moments, Θ_M, in β-sheets (right) and β-barrels (left). The β-strand tilt is β; the tilt of the barrel or sheet axis, relative to the membrane normal (z), is α. For the amide I band, $\Theta_I = 90° - \beta$, and for the amide II band, $\Theta_{II} = \beta$.

band dichroic ratio, $R(\Theta)$, by (20, 26)

$$\langle P_2(\cos \alpha) \rangle = \frac{E_x^2/E_y^2 - R(\Theta) + E_z^2/E_y^2}{P_2(\cos \Theta)[E_x^2/E_y^2 - R(\Theta) - 2E_z^2/E_y^2]} \quad (1)$$

where E_x, E_y, and E_z are the components of the electric field vector in the sample, normalized to those of the incident infrared beam. The z-axis is normal to the ATR plate, the x-axis lies in the plane of incidence, and the y-axis is orthogonal to the latter. The order parameter is defined in terms of the Legendre polynomial: $\langle P_2(\cos \alpha) \rangle = (1/2) \times (3\langle \cos^2 \alpha \rangle - 1)$, where angular brackets indicate an ensemble average over all amides. The orientation of the amide transition moment, relative to the β-strand axis, is given by $\Theta = 90° - \beta$ for the amide I band and by $\Theta = \beta$ for the amide II band, where β is the tilt angle of the strands to the barrel axis (see left-hand panel of Figure 1). The angle α is the inclination of the barrel axis to the normal to the orienting substrate (i.e., the ATR crystal), and the order parameter is determined by the distribution in α. In the case of partial disorder in alignment of the sample on the substrate, the order parameter, $\langle P_2(\cos \alpha) \rangle$, is the product of the order parameter, $\langle P_2(\cos \alpha) \rangle_o$, of the barrel axis relative to the membrane normal and an order parameter, $S_{disorder}$, that characterizes the misalignment of the membrane. For a model in which a fraction $(1 - f)$ of the sample is totally disordered and the remainder is perfectly ordered, $\langle P_2(\cos \alpha) \rangle = f\langle P_2(\cos \alpha) \rangle_o$ (27).

The dichroism of a flattened β-barrel, or of β-strands extending beyond the barrel domain, may be depicted better in terms of a planar β-sheet. For the latter, the dichroic ratio of the amide I band is given by (19)

$$R_I = \frac{E_x^2}{E_y^2} + \frac{2\langle \cos^2 \alpha \rangle \langle \sin^2 \beta \rangle}{1 - \langle \cos^2 \alpha \rangle \langle \sin^2 \beta \rangle} \frac{E_z^2}{E_y^2} \quad (2)$$

and that of the amide II band by

$$R_{II} = \frac{E_x^2}{E_y^2} + \frac{2\langle \cos^2 \alpha \rangle \langle \cos^2 \beta \rangle}{1 - \langle \cos^2 \alpha \rangle \langle \cos^2 \beta \rangle} \frac{E_z^2}{E_y^2} \quad (3)$$

where α is the inclination of the β-sheet to the normal to

the orienting substrate, and β is the tilt of the β-strands within the β-sheet (see right-hand panel of Figure 1). For a partially oriented sample,

$$\langle \cos^2 \alpha \rangle = f\langle \cos^2 \alpha \rangle_o + (1 - f)/3 \quad (4)$$

where $(1 - f)$ is the fraction unoriented, and $\langle \cos^2 \alpha \rangle_o$ is referred to the membrane normal, just as for the β-barrel case.

MATERIALS AND METHODS

Materials. E. coli strain P.400, expressing wild-type OmpA, was a generous gift from Dr. Ulf Henning, Tübingen, Germany. Wild-type OmpA was isolated and purified from the E. coli outer membrane in the unfolded form in 8 M urea, as described in ref 28. E. coli strain BL21(DE3), carrying plasmid pBk7H and expressing FhuAΔ5-160, was a generous gift from Drs. Helmut Killmann and Volkmar Braun, Tübingen (29). The His$_6$-tagged barrel domain of FhuA, without the cork domain, was extracted from E. coli outer membranes and isolated in N-lauroyl-N,N-dimethylammonium N-oxide (LDAO) detergent micelles, without any unfolding, essentially as described in ref 30, except that minimal medium was used. In addition to ampicillin, the minimal medium also contained kanamycin but not tetracycline. Symmetrical, disaturated phosphatidylcholines with odd and even chain lengths from C(12:0) to C(17:0) were obtained from Avanti Polar Lipids (Alabaster, AL), and all other chemicals were from Sigma Chemical Co. (St. Louis, MO).

Unfolded OmpA was folded into detergent micelles as described in ref 31. Briefly, 500 μL of a 42 mg/mL solution of unfolded OmpA in 10 mM borate, 2 mM EDTA, pH 10 buffer that contained 8 M urea was diluted 20-fold with the borate buffer and mixed with an 800-fold molar excess of LDAO detergent. The mixture was incubated overnight at 40 °C to ensure complete refolding of the protein. Refolding was carried out at pH 10 because a yield of close to 100% is achieved at this pH value (31). Sample purity and folding were monitored by SDS polyacrylamide gel electrophoresis (PAGE) according to the method in ref 32, except that samples were not boiled prior to electrophoresis.

The gene encoding the transmembrane domain of OmpA (amino acid residues 0−176) was amplified via PCR from pET1113 (33), kindly provided by Dr. Tanneke den Blaauwen, University of Amsterdam, The Netherlands. The upstream primer 5′-CGGCAT**ATG**GCTCCGAAAGATAACACCTG-3′ was used to introduce a start codon (underlined) to replace the signal sequence of *proOmpA*, and the downstream primer 5′-CTGCTCGAG**TCA**AGCTGCTTCGCCCTGACCGA-3′ converted the codon for proline 177 to a stop codon (underlined). TCA in the downstream primer corresponds to the reversed complement, TGA, in the *proompA* gene, which is a stop codon. The gene of OmpA (0−176) was then ligated into pET22b (Novagen) using the *Nde*I and *Xho*I restriction enzyme cut sites to yield the plasmid pET22bB1. The plasmid was transformed into E. coli strain BL21(DE3) ΔlamB ΔompF::Tn5 ΔompA ΔompC ΔfhuA (34) using the protocol "One-step preparation and transformation of competent cells" (35). OmpA (0−176) was subsequently purified as described in refs 28 and 36.

For refolding of the transmembrane domain of OmpA, 12 mg of denatured OmpA(0−176) was diluted into 20 mL of 25 mM LDAO in 10 mM borate buffer containing 2 mM EDTA (pH 10). The proteins were incubated at 40 °C for 12 h. The yield of refolding was 100%, as confirmed by SDS−PAGE and CD spectroscopy. In SDS−PAGE, OmpA0−176 displayed the typical band-shift from 19 kDa (unfolded) to 23 kDa (folded form), as observed previously (36), if samples were not boiled prior to electrophoresis. The full-length wt-OmpA similarly displayed a band-shift from 35 kDa to 30 kDa in SDS−PAGE, as described previously (28), if samples were not heat-denatured prior to electrophoresis. Folding was quantitative, because the bands for the unfolded proteins disappeared after refolding but appeared again when samples were boiled (heat-denatured) in SDS prior to electrophoresis. After refolding, OmpA was concentrated 20-fold in an Amicon ultrafiltration chamber using Amicon YM-10 membranes.

Reconstitution into Membranes. Lipid stock solutions were prepared in $CHCl_3$ and dried under a stream of dry nitrogen gas. The resulting lipid film was desiccated overnight under vacuum and then covered with argon. The dry lipid film was hydrated with 10 mM Hepes, 2 mM EDTA buffer, pH 7.0, and frozen (in liquid nitrogen) and thawed (in a water bath at ∼5° above the transition temperature of the phospholipid) seven times to obtain uniform lipid vesicles.

The reconstitution was carried out by mixing 1 mg of the above lipid vesicles with protein to the desired lipid−protein ratio, and then 10% sodium cholate solution was added to give a final concentration of 0.2% sodium cholate in a total volume of 500 μL. The sample was mixed well and incubated at room temperature for 1 h, vortexing from time to time. After 1 h of incubation, the protein was precipitated with 52.5% ammonium sulfate solution that was added to 35% final concentration. The pellet containing the reconstituted protein was then centrifuged for 30 min at 35000 rpm in a 50TI rotor.

The pellet contains the reconstituted sample, and because the outer-membrane proteins have a low density, the reconstituted membrane pellets tend to float when centrifuged. This decreases the protein and lipid content and invariably changes the lipid−protein (L/P) ratios from the expected range. L/P ratios were therefore determined after ammonium sulfate precipitation (37, 38), and then the samples were adjusted to achieve a L/P ratio close to 50 mol/mol by adding solubilized lipid vesicles. The pellet was dissolved and vortexed in 500 μL of 10 mM Hepes buffer pH 7.0, containing 2 mM EDTA and 250 mM NaCl. Detergent removal was achieved by extensive dialysis at 8 °C against 10 mM Hepes buffer pH 7.0, containing 2 mM EDTA and 250 mM NaCl, using 10-kDa cutoff dialysis membranes. Four or five changes of 2 L of buffer were made every 7−8 h, with the last dialysis step overnight.

ATR Spectroscopy. OmpA was purified and reconstituted as described above. The reconstituted sample was layered on a clean ZnSe ATR crystal. Initially, the sample was dried with dry nitrogen purge and then desiccated overnight with a vacuum pump. The dry lipid film was incubated in a Bruker IFS 25 FTIR spectrometer by purging with dry nitrogen at 1.5 kp/cm² pressure. ATR spectra were recorded at a nominal resolution of 2 cm⁻¹ with parallel and perpendicular polarization of the incident beam. The sample was then hydrated
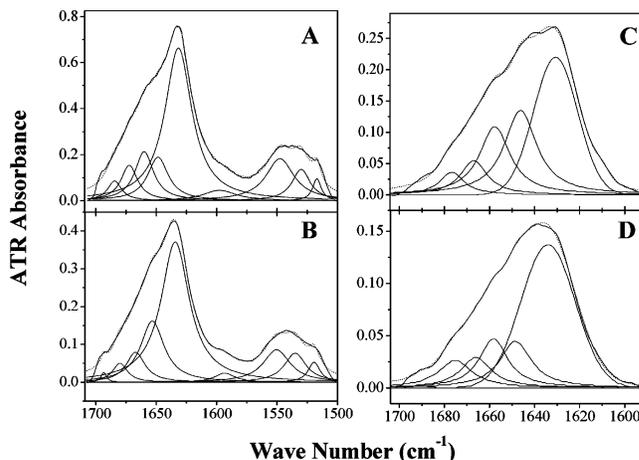
FIGURE 2: Polarized ATR-FTIR spectra of OmpA reconstituted with ditridecanoyl phosphatidylcholine lipid. Spectra A and B are obtained in the dry state, whereas spectra C and D are obtained in the hydrated fluid phase. The spectra in the upper panels (A, C) correspond to parallel polarization, and those in the lower panels (B, D) correspond to perpendicular polarization, of the incident radiation. Note the different ordinate scales. The dotted lines correspond to the theoretical fit, with the bands obtained from the band-fitting analysis shown below the experimental spectrum.

with 10 mM Hepes pH 7.0 buffer containing 2 mM EDTA and 250 mM NaCl, prepared in D_2O, and washed (using a pipet) again with the same buffer in order to remove noninserted lipid and protein (23). Meanwhile, ATR spectra were recorded at both polarizations for every wash. The sample holder was temperature controlled using a recirculating water bath, and the spectra were recorded in the gel phase (∼10° below the lipid chain melting temperature) and in the fluid phase (∼10° above the lipid chain melting temperature) of the membranes. Further details of the ATR spectroscopy are given in ref *39*.

To determine the dichroic ratio, each spectrum was analyzed using OPUS Version 3.02 software from Bruker (Karlsruhe, Germany). If necessary, spectra were smoothed with 11-point Savitsky−Golay smoothing to remove the noise from the residual water vapor. A local baseline was established, and curve fitting using the Levenberg−Marquardt algorithm was carried out from 1500 to 1708 cm⁻¹ and from 1600 to 1700 cm⁻¹ for dry and hydrated samples, respectively. The intensity ratios of parallel and perpendicular polarization were taken as the ATR dichroic ratio (*R*) from the intensities obtained at 1630 and 1530 cm⁻¹ from the curve-fitting analysis for the amide I and amide II bands, respectively. The dichroic ratio changes with the first two to three washes and then becomes stable, which is taken to correspond to the respective hydrated samples. To calculate molecular orientations from dichroic ratios, intensities of the infrared electric field components were obtained from the thick film approximation: $E_x^2/E_y^2 = 0.450$ and $E_z^2/E_y^2 = 1.550$ for a ZnSe ATR crystal (see, e.g., ref *40*).

RESULTS

Outer-Membrane Protein OmpA. Figure 2 shows the amide region from the polarized ATR spectra of OmpA in aligned membranes of ditridecanoyl phosphatidylcholine (diC(13:0)PtdCho). In the dry state (Figure 2A,B), both the amide I and amide II bands are visible, whereas in membranes hydrated with D_2O (Figure 2C,D), the amide II band

Table 1: Band Fitting of the Polarized ATR Spectra from the Amide I Band of OmpA in Hydrated Disaturated Phosphatidylcholines of Different Chain Lengths, C(n:0), in the Gel and Fluid Phases

	gel		fluid	
C(n:0)	position (cm^{-1})	normalized area (%)[a]	position (cm^{-1})	normalized area (%)[a]
C(12:0)			1631	41
			1645	36
			1653	16
			1663	5
			1674	2
C(13:0)	1631	42	1633	49
	1646	30	1645	18
	1657	18	1658	17
	1667	7	1666	9
	1676	3	1676	7
C(14:0)	1631	58	1632	59
	1647	19	1645	10
	1657	14	1653	18
	1665	7	1663	10
	1673	2	1672	3
C(15:0)	1632	56	1633	58
	1645	10	1646	14
	1653	19	1655	15
	1663	11	1663	10
	1673	4	1672	3
C(17:0)	1633	63	1633	56
	1645	7	1652	28
	1655	15	1663	10
	1664	11	1672	5
	1673	4	1682	1

[a] Relative band intensities are obtained by combining integrated absorbances, $A_{\parallel}$ and $A_{\perp}$, with radiation polarized parallel and perpendicular, respectively, to the plane of the incident beam. The appropriate combination that reflects the full intensity is $A_{\parallel} + (2E_z^2/E_y^2 - E_x^2/E_y^2)A_{\perp}$ (42).

is shifted to much lower frequencies, where it overlaps with bands from the lipid. Qualitatively, the band shapes resemble those of other β-barrel outer-membrane proteins in the dry (21) and hydrated (23) states. The band fitting shown in Figure 2 demonstrates the predominant β-sheet content of the protein, with the major band at ca. 1630 cm^{-1} in the amide I region ($\nu_{\perp}(\pi,0)$ mode) and that at ca. 1530$-$1550 cm^{-1} in the amide II region ($\nu_{\parallel}(0,\pi)$ mode). The minor band at ca. 1675 cm^{-1} in the amide I region ($\nu_{\parallel}(0,\pi)$ mode) from hydrated membranes is characteristic of antiparallel β-sheets (41).

Table 1 gives the results of band fitting for the amide I region from OmpA in disaturated phosphatidylcholines of different chain lengths. Fitting data are given for hydrated membranes in the gel and fluid phases, recorded at temperatures 10° below and 10° above the respective chain melting transitions. [Transition temperatures for diC(12:0), diC(13:0), diC(14:0), diC(15:0), and diC(17:0) PtdChos are -2, 14, 23, 34, and 48 °C, respectively (44).] To obtain the true absorbed intensity that reflects relative populations in aligned samples, it is necessary to combine absorbances, $A_{\parallel}$ and $A_{\perp}$, for parallel and perpendicular polarized radiation (42). The appropriate admixture with $A_{\perp}$ in the present geometry is $A_{\parallel} + (2E_z^2/E_y^2 - E_x^2/E_y^2)A_{\perp}$. This is used to calculate the percentage populations that are presented in Table 1. Generally speaking, the populations are rather similar in the different lipid hosts
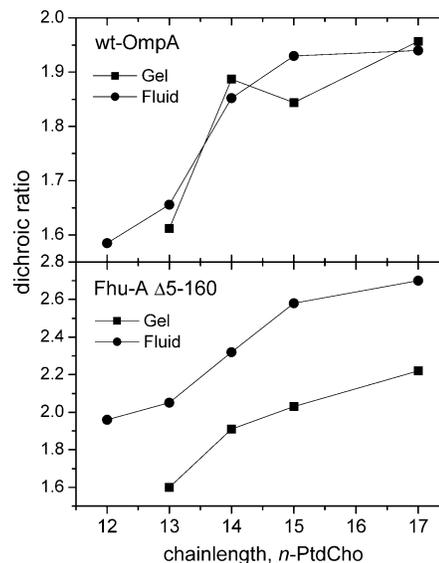
FIGURE 3: Dependence of the dichroic ratios from the amide I band of OmpA (upper panel) and of FhuA barrel domain (lower panel) on chain length, n, of the disaturated phosphatidylcholine membrane in which the protein is incorporated. Dichroic ratios are given for samples in the gel phase (squares) and in the fluid phase (circles). Membranes are hydrated in D$_2$O buffer.

and in the fluid and gel phases. There is, however, a tendency to decrease in β-sheet population at shorter chain lengths, with a corresponding increase in the 1645 cm^{-1} band corresponding to disordered structures. With the exception of diC(12:0)PtdCho, the mean β-sheet population of OmpA in the different lipid hosts is 59 ± 6%, from Table 1, for hydrated membranes. For comparison, the β-sheet content of OmpA truncated to residues 22$-$192 is 63% from the crystal structure (4); (PDB 1QJB). This is similar to the values obtained in the longer lipid hosts. The full-length protein has 325 residues. Therefore, an appreciable part (ca. 55%) of the sizable periplasmic domain must also be β-sheet. For comparison, the resolved 127 residues from the homologous C-terminal domain of RmpM (which shares 35% sequence identity with the periplasmic C-terminal domain of OmpA) contains 25% β-strands and 25% β-turns (43).

From the dichroic ratios of the amide I and amide II bands of the dry sample, it is possible to determine the tilt, β, of the β-strands within the β-sheet. From eqs 2 and 3 for a β-sheet, one obtains a consistent mean value of $\beta = 46.2 \pm 0.8°$ ($N = 5$) from measurements in disaturated phosphatidylcholines of different chain lengths from C12 to C17. Analysis according to eq 1 for axially symmetric barrels yields a similar value for the strand tilt: $\beta = 48° \pm 5°$, averaged over membranes with host lipids of different chain lengths. For the barrel domain alone of OmpA, a somewhat smaller value of $\beta = 43.9 \pm 0.9°$ ($N = 5$) is obtained for the mean strand tilt.

The upper panel of Figure 3 shows the dichroic ratios of the amide I band from OmpA in bilayer membranes hydrated in D$_2$O as a function of chain length of the disaturated phosphatidylcholine. Values are given for membranes in the gel phase and for those in the fluid phase above the lipid chain melting temperature. The general trend is an increase in amide I dichroic ratio with increasing lipid chain length. Use of eq 2, together with the mean value of the strand tilt, β, deduced from the dichroic ratio of the dry sample, yields

Table 2: Order Parameters, $\langle P_2(\cos\alpha)\rangle$, and Mean Effective Inclinations, α, of the β-Sheets of OmpA Reconstituted in Disaturated Phosphatidylcholines, diC(n:0)PtdCho, with Different Chain Lengths, n, in the Gel and Fluid Phases

	gel		fluid	
C(n:0)	$\langle P_2(\cos\alpha)\rangle$	α (deg)	$\langle P_2(\cos\alpha)\rangle$	α (deg)
C(12:0)			0.26 (0.25)[b]	45 (45)[b]
C(13:0)	0.32 (0.35)[b]	42 (41)[b]	0.34 (0.30)[b]	42 (43)[b]
C(14:0)[a]	0.40 (0.52)[b]	39 (35)[b]	0.39 (0.53)[b]	40 (34)[b]
C(15:0)	0.39 (0.51)[b]	40 (35)[b]	0.42 (0.57)[b]	38 (32)[b]
C(17:0)	0.43 (0.62)[b]	38 (30)[b]	0.42 (0.61)[b]	38 (30)[b]

[a] For full-length OmpA, data obtained with 10% dimyristoylphosphatidylglycerol in dimyristoylphosphatidylcholine host matrix. [b] Values in parentheses are obtained with the barrel domain of OmpA (residues 0−176).

the values for the order parameter, $\langle P_2(\cos\alpha)\rangle$, and mean tilt, α, of the β-sheets that are given in Table 2. The trend is similar to that of the dichroic ratios: the order parameters increase, and the tilt angles decrease, with increasing lipid chain length. The differences in order parameters between gel- and fluid-state membranes are not large. Previous ATR measurements on full-length OmpA in single supported bilayers of diC(14:0)PtdCho at room temperature (*23*) yield comparable degrees of order when analyzed by the present methods ($\langle P_2(\cos\alpha)\rangle = 0.35-0.38$). Measurements on diC-(16:0)PtdCho from the same work are also consistent with the present observed trends with chain length for phosphatidylcholines in the gel phase. Conclusions similar to those drawn from Table 2 can also be deduced by analyzing the dichroic ratios according to eq 1 for cylindrical β-barrels. The net values for the tilt, α, of the barrel are considerably larger, however, than those given in Table 2. Note that these values include the tilt of the β-strands in the periplasmic domains, in addition to that of the transmembrane β-barrel.

Experiments were also performed with a truncated form of OmpA, consisting of residues 0−176, that corresponds essentially to the transmembrane barrel domain. Order parameters and effective values for the tilt of the barrel axis are given by the values in parentheses in Table 2. The order parameters are higher (and the tilt angles corresponding are lower) for the barrel domain of OmpA than for the full-length protein, at least in the lipids of longer chain lengths.

The effective tilt angles, θ, of the lipid chains, relative to the substrate normal, are given in Table 3. These values are derived from the dichroic ratios of the CH_2 symmetric and antisymmetric stretch bands at 2851 and 2921 cm^{-1}, respectively. Equation 1 is used for the order parameter of the lipid chains (with $\theta \equiv \alpha$), where the orientation of the transition moment for the CH_2 stretch vibrations is $\Theta = 90°$. Essentially consistent values for θ are obtained from the symmetric and antisymmetric stretch bands. In the gel phase, the values of θ represent the tilt of the long axis of the nearly all-*trans* chains. (In the fluid phase, θ is an effective value that corresponds to the mean order parameter of the individual chain segments that are undergoing rotational isomerism.) For comparison, the tilt of the chains of disaturated phosphatidylcholines in gel-phase bilayers that is determined from X-ray diffraction lies in the range $\theta = 30-35°$ (*44*). The values of θ that are found for the gel-phase membranes in Table 3 are of a similar size and therefore suggest that the OmpA-containing membranes are reasonably well aligned.

Table 3: Effective Tilt, θ (deg), of Lipid Chains in Aligned Membranes of Disaturated Phosphatidylcholines, diC(n:0)PtdCho, Containing Either OmpA or FhuA

	θ_s (2851 cm^{-1})[a]		θ_{as} (2921 cm^{-1})[b]	
C(n:0)	gel	fluid	gel	fluid
OmpA				
C(12:0)		41 (37)[c]		41 (38)[c]
C(13:0)	27 (33)[c]	40 (33)[c]	29 (32)[c]	42 (35)[c]
C(14:0)	23 (32)[c]	28 (36)[c]	28 (34)[c]	32 (40)[c]
C(15:0)	41 (31)[c]	38 (37)[c]	41 (33)[c]	40 (38)[c]
C(17:0)	31 (33)[c]	30 (42)[c]	33 (35)[c]	32 (44)[c]
FhuA				
C(12:0)		43		44
C(13:0)	28	43	26	42
C(14:0)	22	24	26	27
C(15:0)	30	41	33	43
C(17:0)	27	45	30	46

[a] Deduced from the dichroism of the CH_2 symmetric stretch band at 2851 cm^{-1}. [b] Deduced from the dichroism of the CH_2 antisymmetric stretch band at 2921 cm^{-1}. [c] Values in parentheses are for the reconstituted barrel domain of OmpA.
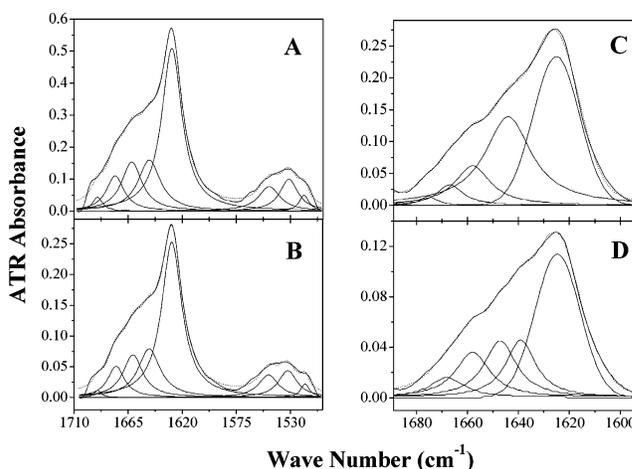
FIGURE 4: Polarized ATR-FTIR spectra of the β-barrel domain of FhuA reconstituted with dipentadecanoyl phosphatidylcholine lipid. Spectra A and B are obtained in the dry state, whereas spectra C and D are obtained in the hydrated gel phase. The spectra in the upper panels (A, C) correspond to parallel polarization, and those in the lower panels (B, D) correspond to perpendicular polarization, of the incident radiation. Note the different ordinate scales. The dotted lines correspond to the theoretical fit, with the bands obtained from the band-fitting analysis shown below the experimental spectrum.

Outer-Membrane Iron Siderophore Receptor FhuA. Figure 4 shows the polarized ATR spectra of the FhuA barrel domain in aligned membranes of dipentadecanoyl phosphatidylcholine. The amide I bands are particularly sharp in the dry state. The low-intensity $\nu_{\parallel}(0,\pi)$ mode of the antiparallel β-sheet at ca. 1695 cm^{-1} is readily visible, in addition to the high-intensity $\nu_{\perp}(\pi,0)$ mode at ca. 1630 cm^{-1}. Intermediate bands correspond to β-turns and unordered loops. Considerably broader amide I bands are obtained for the hydrated membranes, even in the gel phase. This corresponds to an increase in the protein dynamics, compared with those in the dry state. The overall band frequencies and secondary structure are, however, conserved.

Table 4 gives the results of band fitting for the amide I region from FhuA in hydrated membranes of disaturated phosphatidylcholines with different chain lengths. The β-sheet population displays a pattern similar to that found

Table 4: Band Fitting of the Polarized ATR Spectra from the Amide I Band of FhuA in Hydrated Disaturated Phosphatidylcholines of Different Chain Lengths, C(n:0), in the Gel and Fluid Phases

	gel		fluid	
C(n:0)	position (cm^{-1})	normalized area (%)[a]	position (cm^{-1})	normalized area (%)[a]
C(12:0)			1625	40
			1641	29
			1652	21
			1662	8
			1671	2
C(13:0)	1624	48	1626	48
	1640	22	1641	12
	1649	16	1652	19
	1657	9	1662	14
	1666	5	1671	7
C(14:0)	1624	52	1625	52
	1639	12	1642	23
	1647	16	1653	19
	1655	13	1663	4
	1665	7	1669	2
C(15:0)	1625	52	1626	51
	1641	12	1641	11
	1648	18	1648	20
	1658	13	1658	12
	1667	5	1667	6
C(17:0)	1625	48	1626	46
	1640	17	1643	27
	1647	16	1651	14
	1656	12	1660	9
	1665	7	1668	4

[a] Relative band intensities are obtained by combining integrated absorbances, $A_{\parallel}$ and $A_{\perp}$, with radiation polarized parallel and perpendicular, respectively, to the plane of the incident beam. The appropriate combination that reflects the full intensity is $A_{\parallel} + (2E_z^2/E_y^2 - E_x^2/E_y^2)A_{\perp}$ (*42*).

with OmpA in the same lipids, with a small decrease at shorter chain lengths. The effective β-sheet population is slightly less than that of OmpA. With the exception of diC-(12:0)PtdCho, the mean β-sheet population deduced for the β-barrel domain of FhuA in the different lipids of Table 3 is 55 ± 3%. For comparison, the β-sheet content for residues 161−723 that is deduced from the crystal structure of FhuA is 63% (*45*) (PDB 1QFG).

The lower panel of Figure 3 shows the dependence on lipid chain length of the amide I dichroic ratios for the β-barrel domain of FhuA. The dichroic ratios increase progressively with increasing chain length of the reconstituting disaturated phosphatidylcholine phospholipid. From the amide I and amide II dichroic ratios of the dry samples, a consistent mean tilt of $\beta = 44.5 \pm 0.7°$ ($N = 5$) can be deduced from measurements in phosphatidylcholines of chain lengths from C(12:0) to C(17:0) by using eqs 2 and 3. Together with this value, the order parameters and mean tilts of the β-sheets of FhuA that are obtained from the amide I dichroic ratios by using eq 2 are given in Table 5. Similar to the situation with OmpA, the orientation of FhuA improves progressively with increasing chain length of the reconstituting lipid. However, the degree of orientation of FhuA is considerably greater in the fluid phase than in the gel phase, unlike for OmpA. Also, the order parameters for FhuA are greater than those for OmpA in the same lipid system, in both fluid and gel phases. Again, analysis of the amide

Table 5: Order Parameters, $\langle P_2(\cos \alpha) \rangle$, and Mean Effective Inclinations, α, of the β-Sheets of FhuA Reconstituted in Disaturated Phosphatidylcholines, diC(n:0)PtdCho, with Different Chain Lengths, n, in the Gel and Fluid Phases

	gel		fluid	
C(n:0)	$\langle P_2(\cos \alpha) \rangle$	α (deg)	$\langle P_2(\cos \alpha) \rangle$	α (deg)
C(12:0)			0.48	36
C(13:0)	0.31	43	0.51	35
C(14:0)	0.48	36	0.65	29
C(15:0)	0.57	33	0.79	22
C(17:0)	0.63	30	0.80	21

dichroism according to eq 1 for axially symmetric barrels leads to similar conclusions. The mean strand tilt in the different host lipids is $\beta = 42 \pm 4°$, similar to that obtained with the β-sheet formalism, but the order parameters for the barrel axis are considerably lower.

Table 3 gives the effective tilt angles of the lipid chains for the various phosphatidylcholine membranes containing FhuA. As for membranes containing OmpA, the effective chain tilts in the gel phase are similar to those in gel-phase phosphatidylcholine bilayers. This suggests that the membranes containing FhuA are also reasonably well oriented.

DISCUSSION

Measurements from the amide infrared dichroism yield consistent values for the β-strand tilt in the different phosphatidylcholine lipid hosts. A somewhat larger value of the strand tilt ($\beta \approx 46 \pm 1°$) was obtained for OmpA than for FhuA ($\beta \approx 44.5 \pm 1°$). For comparison, the mean value of the strand tilt derived from the value of $\langle \cos^2 \beta \rangle$ calculated using the crystal structure of OmpA (PDB 1QJP) is $\beta = 43.1°$ (*2*). This latter value includes only residues 1−171 of native mature OmpA (*4*), without the comparably large periplasmic domain that constitutes residues 172−325, and is closer to the value of $\beta = 44 \pm 1°$ obtained here for OmpA, also truncated to residues 0−176. In the case of FhuA, a mean value of $\beta = 38.3°$ (*2*) was obtained from the crystal structure (PDB 2FCP) for the β-barrel domain comprising residues 161−723 (*13*). This is significantly smaller than the value of the strand tilt obtained for FhuA truncated to the barrel domain from infrared dichroism. To the extent that the truncated barrel domain represents the whole protein, the somewhat larger tilt obtained in membranes may represent a slight relaxation of the FhuA barrel structure, relative to packing of the whole protein in the crystal. Correspondingly, from the change in bandwidths in Figures 2 and 4, a greater flexibility of the protein structure is evidenced in the hydrated membrane than in the dry membrane.

Unfortunately, it is not possible to measure the dichroic ratio of the amide II band reliably in the hydrated state. Therefore, we used the strand tilt determined from the dry samples to deduce the order parameter of the protein in hydrated membranes. The above considerations suggest that this might introduce some uncertainty into the values obtained for the order parameter. However, this is less likely to affect the dependence of the protein order parameter on lipid chain length. (Note that the strand tilt determined in the dry state is independent of chain length.)

The values obtained for the strand tilt, β, from the polarized ATR measurements can be used to obtain estimates

of the sheet twist, θ, and the strand coiling, ϵ, by using the expressions derived for idealized β-barrels (46):

$$\theta = \frac{\theta_o + \frac{2\pi}{n}\left[\left(\frac{h}{d}\right)^2 \frac{\cos\beta}{\tan\beta} + \sin\beta\right]}{\left(\frac{h}{d}\right)^2 \frac{1}{\tan^2\beta} + \frac{1}{\cos^2\beta}} \qquad (5)$$

and

$$\epsilon = \left(\frac{h}{d}\right)\left(\frac{2\pi}{n} - \frac{\theta}{\sin\beta}\right)\cos\beta \qquad (6)$$

where the number of strands is $n = 8$ and 22 for OmpA and FhuA, respectively. Optimized values for the twist in an unstrained sheet of long strands, and for the characteristic dimensions of a β-sheet in this model are $\theta_o = -3.4°$ and $h/d = 0.719$, respectively (2). This yields values for the twist of $\theta = 18°$ and for the coiling of $\epsilon = 10°$ from the IR dichroism of OmpA in lipid membranes. For comparison, the twist and coiling angles obtained from the X-ray coordinates of crystalline OmpA are $\theta = 18.1°$ and $\epsilon = 12.0°$ (see ref 2). For the FhuA barrel domain, $\theta = 6°$ and $\epsilon = 4°$ from IR dichroism, as compared with $\theta = 6.8°$ and $\epsilon = 3.5°$ deduced from the X-ray coordinates (2). The barrel geometry is therefore similar in the two environments.

The crystal structure (47) or hydropathy analysis (48) of the OmpA transmembrane barrel shows that the hydrophobic belt and aromatic girdles comprise an average of five outward-facing residues in each of the eight strands of the β-barrel. With a mean strand tilt of $44 \pm 1°$, the transmembrane thickness of this hydrophobic stretch is therefore predicted to be $10h\cos\beta = 2.5 \pm 0.05$ nm, where $h = 0.345$ nm (49) is the rise per residue in an antiparallel β-sheet. This agrees well with recent estimates for a range of β-barrel proteins from the *E. coli* outer membrane (50).

Whereas there is little systematic change in lipid order with lipid chain length (see Table 3), progressive changes are found in the protein orientation (see Tables 2 and 4). The increasing orientational order, or decreasing tilt, of the β-barrels with increasing chain length of the host phosphatidylcholine lipid therefore arises undoubtedly from hydrophobic matching (or mismatching) between the protein and lipid. The tilt of the barrel will be reduced when the hydrophobic span of the lipid bilayer increases relative to that of the protein, and will increase when the lipid bilayer thickness decreases. The greater orientational freedom of OmpA in diC(12:0)PtdCho than in phosphatidylcholines with longer chains correlates well with the optimal folding and insertion of OmpA into large unilamellar vesicles composed of this lipid (25). The membrane ordering of FhuA is greater than that of OmpA, in the fluid phase of any particular lipid host. This presumably is the result of the difference in barrel size. FhuA has cross-sectional dimensions 3.9 nm × 4.6 nm (13) that considerably exceed the membrane thickness, whereas OmpA has an outer diameter of ca. 2.4 nm (47). In the gel phase, however, the order of FhuA is more comparable to that of OmpA, most probably because the protein ordering is dominated in both cases by that of the close-packed all-*trans* lipid chains.

For the trimeric β-barrel porin OmpF from *E. coli*, the lipid binding constants of di-*cis*-monounsaturated phosphati-

dylcholines have been measured as a function of lipid chain length by competition experiments with brominated dioleoyl phosphatidylcholine (51). A maximum in affinity was found for diC(14:1)PtdCho, with a progressive decrease for longer chain lengths. In the latter regime, the lipid hydrophobic thickness is expected to exceed that of the protein, which is consistent with the increasing order of OmpA and FhuA with increasing chain length. Note that a maximum in ordering of the protein is not expected under conditions of hydrophobic matching. In a single-component lipid system, the protein order will either increase or remain constant as the hydrophobic length of the lipid exceeds that of the protein.

The bilayer thickness for a diunsaturated lipid is less than that for a disaturated lipid of equal chain length (52). Consequently, the bilayer thickness of diC(14:1)PtdCho is comparable to that of diC(12:0)PtdCho for the disaturated lipids used in this study. Extrapolation of the optimized data given in ref 53 for diC(14:0)PtdCho, diC(16:0)PtdCho, and diC(18:1)PtdCho predicts a hydrophobic thickness of $2D_c = 2.4$ nm for diC(12:0)PtdCho and $2D_c = 2.3$ nm for diC-(14:1)PtdCho. Thus, the monotonic increase in ordering of OmpA and FhuA with lipid chain length (Tables 2 and 5) is consistent with the chain length dependence of the lipid affinities for OmpF. The highest affinity, i.e., best matching, is found for a bilayer hydrophobic thickness of 2.3 nm, which corresponds to diC(12:0)PtdCho in the saturated phosphatidylcholine series. From the crystal structures, it has been deduced that the hydrophobic thicknesses of OmpA, OmpF, and FhuA are each ca. 2.4 nm (50). This presumably corresponds to the hydrophobic thickness of the *E. coli* outer membrane that is reasonably well mimicked by diC(12:0)-PtdCho or diC(14:1)PtdCho, according to the data in ref 53.

It is worth noting, however, that extrapolation of the X-ray scattering data of ref 52 yields estimates of 2.15 and 1.95 nm for the hydrophobic thicknesses of diC(14:1)PtdCho and diC(12:0)PtdCho bilayer membranes, respectively. Until now, this latter, more extensive data set has been used routinely in the discussion of hydrophobic matching. These lower values would imply that diC(14:1)PtdCho and diC(12:0)-PtdCho bilayers are appreciably shorter than the hydrophobic thickness of the *E. coli* outer membrane. According to ref 52, the hydrophobic thickness of diC(14:0)PtdCho is 2.3 nm. This would correlate better with the chain length dependence of the infrared order parameters that is given in Tables 2 and 5. The onset of maximum ordering, which presumably corresponds to achieving hydrophobic matching, occurs for phosphatidylcholine chain lengths C(14:0)−C(15:0). Significantly, the lipopolysaccharide component of the outer membrane is characterized by relatively short chains, both C12 and C14 (54).

It is significant to note that recent simulations of OmpA and OmpT in dimyristoyl phosphatidylcholine bilayers by means of molecular dynamics have revealed a dynamic tilt of the β-barrel axis relative to the membrane normal (55, 56). A tilt of ca. 5−10° was detected for OmpA and of ca. 20° for OmpT, although the duration of the simulation was probably insufficient to ensure a true thermodynamic average for this cooperative motion of the lipids plus protein. Because this represents a rigid body motion, off-axis rotations of finite amplitude are likely to be a general feature of small transmembrane proteins, including α-helical bundles. In the latter case, infrared dichroism cannot distinguish off-axis

motion from the static tilt of individual helices relative to the protein symmetry axis (*20*). This dynamic feature of protein incorporation into fluid lipid membranes may have functional significance. Our results with FhuA indicate that such effects will be less important for larger transmembrane proteins.

REFERENCES

1. Schulz, G. E. (2002) The structure of bacterial outer membrane proteins, *Biochim. Biophys. Acta 1565*, 308−317.
2. Páli, T., and Marsh, D. (2001) Tilt, twist and coiling in β-barrel membrane proteins: relation to infrared dichroism, *Biophys. J. 80*, 2789−2797.
3. Vogt, J., and Schulz, G. E. (1999) The structure of outer membrane protein OmpX from *Escherichia coli* reveals possible mechanisms of virulence, *Struct. Fold. Des. 7*, 1301−1309.
4. Pautsch, A., and Schulz, G. E. (2000) High-resolution structure of the OmpA membrane domain, *J. Mol. Biol. 298*, 273−282.
5. Snijder, H. J., Ubarretxena-Belandia, I., Blaauw, M., Kalk, K. H., Verheij, H. M., Egmond, M. R., Dekker, N., and Dijkstra, B. W. (1999) Structural evidence for dimerization-regulated activation of an integral membrane phospholipase, *Nature 401*, 717−721.
6. Weiss, M. S., and Schulz, G. E. (1992) Structure of porin refined at 1.8 Å resolution, *J. Mol. Biol. 227*, 493−509.
7. Kreusch, A., Neubüser, A., Schiltz, E., Weckesser, J., and Schulz, G. E. (1994) Structure of the membrane channel porin from *Rhodopseudomonas blastica* at 2.0 Å resolution, *Protein Sci. 3*, 58−63.
8. Cowan, S. W., Schirmer, T., Rummel, G., Steiert, M., Ghosh, R., Pauptit, R. A., Jansonius, J. N., and Rosenbusch, J. P. (1992) Crystal structures explain functional properties of two *E. coli* porins, *Nature 358*, 727−733.
9. Dutzler, R., Rummel, G., Alberti, S., Hernández-Allés, S., Phale, P. S., Rosenbusch, J. P., Benedi, V. J., and Schirmer, T. (1999) Crystal structure and functional characterization of OmpK36, the osmoporin of *Klebsiella pneumoniae*, *Structure 7*, 425−434.
10. Schirmer, T., Keller, T. A., Wang, Y.-F., and Rosenbusch, J. P. (1995) Structural basis for sugar translocation through maltoporin channels at 3.1 Å resolution, *Science 267*, 512−514.
11. Meyer, J. E. W., Hofnung, M., and Schulz, G. E. (1997) Structure of maltoporin from *Salmonella typhimurium* ligated with a nitrophenyl-maltotrioside, *J. Mol. Biol. 266*, 761−775.
12. Forst, D., Welte, W., Wacker, T., and Diederichs, K. (1998) Structure of the sucrose-specific porin ScrY from *Salmonella typhimurium* and its complex with sucrose, *Nat. Struct. Biol. 5*, 37−46.
13. Ferguson, A. D., Hofmann, E., Coulton, J. W., Diederichs, K., and Welte, W. (1998) Siderophore-mediated iron transport: crystal structure of FhuA with bound lipopolysaccharide, *Science 282*, 2215−2220.
14. Buchanan, S. K., Smith, B. S., Venkatramani, L., Xia, D., Esser, L., Palnitkar, M., Chakraborty, R., van der Helm, D., and Deisenhofer, J. (1999) Crystal structure of the outer membrane active transporter FepA from *Escherichia coli*, *Nat. Struct. Biol. 6*, 56−63.
15. Arora, A., Abildgaard, F., Bushweller, J. H., and Tamm, L. K. (2001) Structure of outer membrane protein A transmembrane domain by NMR spectroscopy, *Nat. Struct. Biol. 8*, 334−338.
16. Fernández, C., Hilty, C., Bonjour, S., Adeishvili, K., Pervushin, P., and Wüthrich, K. (2001) Solution NMR studies of the integral membrane proteins OmpX and OmpA from *Escherichia coli*, *FEBS Lett. 504*, 173−178.
17. Fernández, C., Hilty, C., Wider, G., and Wüthrich, K. (2002) Lipid−protein interactions in DHPC micelles containing the integral membrane protein OmpX investigated by NMR spectroscopy, *Proc. Natl. Acad. Sci. U.S.A. 99*, 13533−13537.
18. Hwang, P. M., Choy, W.-Y., Lo, E. I., Chen, L., Forman-Kay, J. D., Raetz, C. R. H., Privé, G. G., Bishop, R. E., and Kay, L. E. (2002) Solution structure and dynamics of the outer membrane enzyme PagP by NMR, *Proc. Natl. Acad. Sci. U.S.A. 99*, 13560−13565.
19. Marsh, D. (1997) Dichroic ratios in polarized Fourier transform infrared for nonaxial symmetry of β-sheet structures, *Biophys. J. 72*, 2710−2718.
20. Marsh, D. (1998) Nonaxiality in infrared dichroic ratios of polytopic transmembrane proteins, *Biophys. J. 75*, 354−358.
21. Nabedryk, E., Garavito, R. M., and Breton, J. (1988) The orientation of β-sheets in porin. A polarized Fourier transform infrared spectroscopic investigation, *Biophys. J. 53*, 671−676.
22. Goormaghtigh, E., Cabiaux, V., and Ruysschaert, J.-M. (1990) Secondary structure and dosage of soluble and membrane proteins by attenuated total reflection Fourier-transform infrared spectroscopy on hydrated films, *Eur. J. Biochem. 193*, 409−420.
23. Rodionova, N. A., Tatulian, S. A., Surrey, T., Jähnig, F., and Tamm, L. K. (1995) Characterization of two membrane-bound forms of OmpA, *Biochemistry 34*, 1921−1929.
24. Abrecht, H., Goormaghtigh, E., Ruysschaert, J.-M., and Homblé, F. (2000) Structure and orientation of two voltage-dependent anion-selective channel isoforms—an attenuated total reflection Fourier-transform infrared spectroscopy study, *J. Biol. Chem. 275*, 40992−40999.
25. Kleinschmidt, J. H., and Tamm, L. K. (2002) Secondary and tertiary structure formation of the β-barrel membrane protein OmpA is synchronized and depends on membrane thickness, *J. Mol. Biol. 324*, 319−330.
26. Tamm, L. K., and Tatulian, S. A. (1997) Infrared spectroscopy of proteins and peptides in lipid bilayers, *Q. Rev. Biophys. 30*, 365−429.
27. Fraser, R. D. B. (1953) The interpretation of infrared dichroism in fibrous protein structures, *J. Chem. Phys. 21*, 1511−1515.
28. Surrey, T., and Jähnig, F. (1992) Refolding and oriented insertion of a membrane protein into a lipid bilayer, *Proc. Natl. Acad. Sci U.S.A. 89*, 7457−7461.
29. Braun, M., Killmann, H., and Braun, V. (1999) The β-barrel domain of FhuAΔ5-160 is sufficient for TonB-dependent FhuA activities of *Escherichia coli*, *Mol. Microbiol. 33*, 1037−1049.
30. Ferguson, A. D., Breed, J., Diederichs, K., Welte, W., and Coulton, J. W. (1998) An internal affinity-tag for purification and crystallization of the siderophore receptor FhuA, integral outer membrane protein from *Escherichia coli* K-12, *Protein Sci. 7*, 1636−1638.
31. Kleinschmidt, J. H., Wiener, M. C., and Tamm, L. K. (1999) Outer membrane protein A of *E. coli* folds into detergent micelles, but not in the presence of monomeric detergent, *Protein Sci. 8*, 2065−2071.
32. Laemmli, U. K. (1970) Cleavage of structural proteins during the assembly of the head of bacteriophage T4, *Nature (London) 227*, 680−685.
33. Kleinschmidt, J. H., den Blaauwen, T., Driessen, A. J. M., and Tamm, L. K. (1999) Outer membrane protein A of *Escherichia coli* inserts and folds into lipid bilayers by a concerted mechanism, *Biochemistry 38*, 5006−5016.
34. Prilipov, A., Phale, P. S., van Gelder, P., Rosenbusch, J. P., and Koebnik, R. (1998) Coupling site-directed mutagenesis with high-level expression: large scale production of mutant porins from *E. coli*, *FEMS Microbiol. Lett. 163*, 65−72.
35. Ausubel, F. M., Brent, R., Kinston, R. E., Moore, D. D., Seidman, J. G., Smith, J. A., and Struhl, K. (1999) *Short Protocols in Molecular Biology*, John Wiley & Sons Inc., New York.
36. Pautsch, A., Vogt, J., Model, K., Siebold, C., and Schulz, G. E. (1999) Strategy for membrane protein crystallization exemplified with OmpA and OmpX, *Proteins 34*, 167−172.
37. Lowry, O. H., Rosebrough, N. J., Farr, L., and Randall, R. J. (1951) Protein measurement with the Folin phenol reagent, *J. Biol. Chem. 193*, 265−275.
38. Rouser, G., Fleischer, S., and Yamamoto, A. (1970) Two-dimensional thin layer chromatographic separation of polar lipids and determination of phospholipids by phosphorus analysis of spots, *Lipids 5*, 494−496.
39. Kóta, Z., Páli, T., and Marsh, D. (2004) Orientation and lipid-peptide interactions of gramicidin A in lipid membranes: polarized ATR infrared spectroscopy and spin-label electron spin resonance, *Biophys. J. 86*, 1521−1531.
40. Marsh, D. (1999) Spin label ESR spectroscopy and FTIR spectroscopy for structural/dynamic measurements on ion channels, *Methods Enzymol. 294*, 59−92.
41. Miyazawa, T. (1960) Perturbation treatment of the characteristic vibrations of polypeptide chains in various configurations, *J. Chem. Phys. 32*, 1647−1652.
42. Marsh, D. (1999) Quantitation of secondary structure in ATR infrared spectroscopy, *Biophys. J. 77*, 2630−2637.
43. Grizot, S., and Buchanan, S. K. (2004) Structure of the OmpA-like domain of RmpM from *Neisseria meningitidis*, *Mol. Microbiol. 51*, 1027−1037.
44. Marsh, D. (1990) *Handbook of Lipid Bilayers*, CRC Press, Boca Raton, FL.

45. Ferguson, A. D., Welte, W., Hofmann, E., Lindner, B., Holst, O., Coulton, J. W., and Diederichs, K. (2000) A conserved structural motif for lipopolysaccharide recognition by procaryotic and eucaryotic proteins, *Struct. Fold. Des. 8*, 585−592.

46. Marsh, D. (2000) Infrared dichroism of twisted β-sheet barrels. The structure of *E. coli* outer membrane proteins, *J. Mol. Biol. 297*, 803−808.

47. Pautsch, A., and Schulz, G. E. (1998) Structure of the outer membrane protein A transmembrane domain, *Nat. Struct. Biol. 5*, 1013−1017.

48. Vogel, H., and Jähnig, F. (1986) Models for the structure of outer-membrane proteins of *Escherichia coli* derived from Raman spectroscopy and prediction methods, *J. Mol. Biol. 190*, 191−199.

49. Arnott, S., Dover, S. D., and Elliot, A. (1967) Structure of β-poly-L-alanine: Refined atomic co-ordinates for an anti-parallel beta-pleated sheet, *J. Mol. Biol. 30*, 201−208.

50. Lee, A. G. (2003) Lipid−protein interactions in biological membranes: a structural perspective, *Biochim. Biophys. Acta 1612*, 1−40.

51. O'Keeffe, A. H., East, J. M., and Lee, A. G. (2000) Selectivity in lipid binding to the bacterial outer membrane protein OmpF, *Biophys. J. 79*, 2066−2074.

52. Lewis, B. A., and Engelman, D. M. (1983) Lipid bilayer thickness varies linearly with acyl chain length in fluid phosphatidylcholine vesicles, *J. Mol. Biol. 166*, 211−217.

53. Nagle, J. F., and Tristram-Nagle, S. (2000) Structure of lipid bilayers, *Biochim. Biophys. Acta 1469*, 159−195.

54. Harwood, J. L., and Russell, N. J. (1984) *Lipids in Plants and Microbes*, George Allen and Unwin, London.

55. Bond, P. J., Faraldo-Gomez, J. D., and Sansom, M. S. P. (2004) OmpA: A pore or not a pore? Simulation and modeling studies. *Biophys. J. 83*, 763−775.

56. Baaden, M., and Sansom, M. S. P. (2004) OmpT: Molecular dynamics simulations of an outer membrane enzyme. *Biophys. J. 87*, 2942−2953.